
ELECTROMAGNETIC EMISSION OF COSMIC STRINGS

L.V. ZADOROZHNA, B.I. HNATYK

Taras Shevchenko Kyiv National University, Faculty of Physics

(2, Academician Glushkov Ave., Kyiv 03680, Ukraine; e-mail:

Zadorozhna_Lida@ukr.net, hnatyk@observ.univ.kiev.ua)

PACS 98.80.Cq
©2009

Cosmic strings are one of the types of topological defects which can appear during appropriate phase transitions in the expanding early Universe. Of a particular interest are the superconducting cosmic strings, in which the massless carriers of charge can move without any resistance. It is shown that the superconducting cosmic strings in an intergalactic magnetic field can be powerful sources of nonthermal radiation. We have calculated the spectra of the synchrotron, self-Compton, and inverse Compton emissions of relativistic electrons accelerated on the leading edge of a shock wave around the string. The modern X-ray and gamma-telescopes can register the loops of cosmic strings at a relatively small distance of about 0.1 Mpc. Nevertheless, the near-cusp regions can generate much powerful but appreciably collimated and therefore more scarce impulses.

1. Introduction

Cosmic strings [1–3] represent one of the types of topological defects which can be formed under phase transitions in the early Universe. The last years, a great attention is paid to macroscopic fundamental superstrings with properties close to those of topological defects [4, 5]. Such superstrings can be formed, for example, as residuals of the annihilation of branes in models of brane inflation [6]. In many models of elementary particle physics, the cosmic strings are formed after the inflation, which leads to their influence on the formation of a large-scale structure of the Universe [7, 8].

In the older cosmological models of the formation of a large-scale structure of the Universe, the strings were considered as ones of the candidates causing the formation of initial perturbations [9–12]. In contemporary models, where the cosmic strings arise at the end of the inflation period, the strings contribute insignificantly to the total spectrum of fluctuations of the density [13, 14]. Their contribution is essentially limited by observable data. For example, the fluctuations of the temperature

of the cosmic microwave background (CMB) can be a result of some combinations of quantum fluctuations in the Universe and the perturbations caused by cosmic strings [15–18]. However, no direct observations of strings in fluctuations of the microwave emission are available till now, which imposes some restrictions on the parameters of strings, in particular $G\mu/c^2 \leq 3.2 \times 10^{-7}$, where μ is the tension (or the mass per unit length) of a string, G is the gravitational constant, and c is the light velocity [19].

For the time of their existence, the strings have formed entangled networks which are composed of loops and infinite strings [20, 21]. The strings oscillate and move with relativistic velocities. When the strings cross one another, they are reclosed; the self-intersection leads to the creation of closed loops. The numerical calculations of the evolution of strings indicate that the network of strings evolves in a scale-invariant way which is characterized by the presence of several infinite (in the limits of the horizon) segments and a collection of loops with various lengths in each Hubble volume [22, 23].

An important direction of studies is the gravitational lensing on cosmic strings [24, 25]. In particular, the lensing on infinite cosmic strings gives two identical images of a background object [26, 27]. The lenses-loops of strings can induce a rather strong increase in the luminosity of background stars and can be observed due to this phenomenon [25]. In 2000, F. Bernardeau and J. Uzan [28] notices one more specific feature of the lensing by cosmic strings related to small oscillations on a string. In the vicinity of such a string, a sequence of bright images appearing at the lensing on its substructures will be seen.

In 2003, M. Sazhin *et al.* [29] claimed on the possible discovery of the first case of the lensing on a cosmic string. They observed two galaxies very similar by form and by spectrum which seem to be the images of a single

galaxy formed by the gravitational lensing on a straight cosmic string. However, the special program of observations on the Hubble telescope revealed that these images correspond to two different galaxies [30].

At the present time, several communications about a possible experimental discovery of cosmic strings are known. For example, the authors of work [31] analyzed fluctuations of the brightness of the well-known gravitationally lensed quasar Q0957+561. The object is composed of two images of the quasar which are positioned at a distance of about 6" and are formed due to the gravitational lensing on a massive galaxy. Due to the difference in the paths of rays from different images, the fluctuations in objects A and B are shifted in the time by 412 days. However, on a certain section of the curve of brightness, the synchronous fluctuations of the brightness of both images were revealed. The synchronism of fluctuations of the brightness is explained in [31] by the motion of the loop of a cosmic string near the way of rays from the images to the observer. The gravitational field of loops is periodically varied, due to oscillations, and introduces synchronous fluctuations of the brightness of the quasar image.

There exist also the superconducting cosmic strings, inside of which the massless carriers of charge (zero modes) are present and move, by undergoing no resistance [32–34]. A significant attention is given to the electrodynamic properties of such strings and to their interaction with the cosmic plasma. In the presence of a current along a string, these objects become sources of electromagnetic emission. In this case, the important role is played by the emission of the so-called cusps on a string. Cusps are periodically appearing nonsmooth (like a break) regions of a string, whose vertices reach almost instantaneously the velocity of light. The cusps generate sparks of the electromagnetic emission directed along their motion [35] which can serve a source of energy for some cosmological gamma-sparks [36]. Work [37] reported on the discovery of a millisecond radiospark which was interpreted in [38] as a spark from the cusp on a superconducting cosmic string.

It was shown in [39] that if a superconducting string moves through the cosmic plasma, the former can be observed as a source of the synchrotron emission. In [39], a nonrelativistic string was considered. At the same time, the loops of cosmic strings or separate segments can move with relativistic velocities. In the present work, we will consider the nonthermal (synchrotron and inverse Compton) emission of particles (electrons) of the cosmic plasma accelerated on the front of a relativistic shock wave around a string.

2. Cosmic Strings in a Local Universe

The energy scale of a phase transition is characterized [40, 41] by some dimensionless parameter η related to the mass per unit length (tension) μ of a string by $\mu \sim \eta^2$. The energy loss rate by a string due to the gravitational emission is determined by the parameter

$$\alpha = \frac{\Gamma G \mu}{c^2}, \quad (1)$$

where $\Gamma \sim 50$ is the dimensionless parameter [42]. The typical length of loops is determined by the relation $l = \alpha ct$, where t is the cosmological time moment. Since we consider a close region of the Universe, we may take $t = t_0 = 13.6 \times 10^9$ yr.

The dependence of the concentration distribution function for the loops of strings on the time looks as

$$n = \frac{1}{\alpha(ct)^3}. \quad (2)$$

For a given α , the average distance, on which the loops can be positioned, is $d_s = n^{-1/3} = \alpha^{1/3} ct$. The mean angle $\theta \sim l/d_s = \alpha^{2/3}$, at which the Earth's observer sees a loop, depends only on the type (tension) of a string (see Table 1).

3. Superconducting Strings in Plasma

The motion of strings and loops in the intergalactic plasma is characterized by the parameters: the concentration of protons and electrons $n_e \sim n_p = n_1 = 10^{-7} n_{-7} \text{ cm}^{-3}$, $B_1 = B_{\text{IGM}} = 10^{-7} B_{-7} \text{ Gs}$ is the magnetic field, and IGM means the intergalactic medium. Let a superconducting string move in the intergalactic medium with a Lorentz-factor γ_s .

During oscillations of a loop in the intergalactic magnetic field, an electric current is generated in it with the mean amplitude

$$i = k_i q_e^2 B_{\text{IGM}} l / \hbar. \quad (3)$$

The current generates the proper magnetic field near the string [43]

$$B_{\text{mag}}(r) = 2i/cr, \quad (4)$$

Table 1. Characteristics of strings with various tensions

| α | Parameters of strings | | |
|------------|-----------------------|-------------------|----------|
| | l , (pc) | d_s , (pc) | θ |
| 10^{-6} | 4.2×10^3 | 4.2×10^7 | 21'' |
| 10^{-8} | 42 | 9.1×10^6 | 1'' |
| 10^{-11} | 0.042 | 9.1×10^5 | 0.01'' |

where r is the distance from the string, q_e is the electron charge, \hbar is the Planck constant, and $k_i \sim 1$ is a constant.

The ionized cosmic plasma cannot penetrate into the region with a strong magnetic field near the string. Therefore, at the circumfluence of the string, a shock wave is formed at some distance r_s from it. Behind its front, the flow of the intergalactic plasma in the reference system of the string is decelerated and flows around the “magnetosphere” of the string which is a region with the high pressure of the magnetic field balancing the dynamical pressure of a plasma in the after-shock region on the string. We note that the pressure does not vary on the tangent break (the boundary of the magnetosphere and the after-shock region), and the size (radius) of the magnetosphere is close to the size (radius) of the shock wave, whose velocity relative to the magnetosphere plasma is equal to the velocity of the string. Therefore, the radius of a shock wave can be determined from the condition of equality of the pressure of the magnetic field of the magnetosphere P_{mag} and the pressure behind the front of the relativistic wave P_{dyn} in the reference system of the string: $B_{\text{mag}}^2/8\pi = n_1 m_p c^2 \gamma_{\text{sh}}^2$, where $\gamma_{\text{sh}} = \gamma_s$ is the Lorentz-factor of the shock wave. With the accepted notations ($\alpha_{-8} = \alpha/10^{-8}$, $B_{-7} = B/10^{-7}$, $n_{-7} = n/10^{-7}$), we get

$$r_s = \frac{k_i q_e^2 B_{\text{IGM}} l}{2 \hbar c^2 \gamma_{\text{sh}} \sqrt{\pi n_1 m_p}} = 3.1 \times 10^{15} k_i \gamma_{\text{sh}}^{-1} B_{-7} \alpha_{-8} n_{-7}^{-1/2} \text{ cm.} \quad (5)$$

The geometry of the problem allows us to separate the following regions (see Fig. 1): 1 – unperturbed cosmic plasma, 2 – the plasma behind the front of a shock wave, 3 – behind the boundary of the magnetosphere, the plasma is absent.

4. Acceleration of Electrons on the Front of a Shock Wave

The characteristics of a shock wave (its Lorentz-factor γ_{sh} and the Lorentz-factor of the plasma behind the front of the wave γ_2 ; both are considered in the laboratory reference system) satisfy the relation (Blandford & McKee, 1976)

$$\gamma_2 \simeq \sqrt{(\gamma_{\text{sh}}^2 + 1)}/2. \quad (6)$$

So, for an ultrarelativistic shock wave ($\gamma_{\text{sh}} \gg 1$), we have $\gamma_2 \simeq \gamma_{\text{sh}}/\sqrt{2}$, and the concentration of particles n_2 and

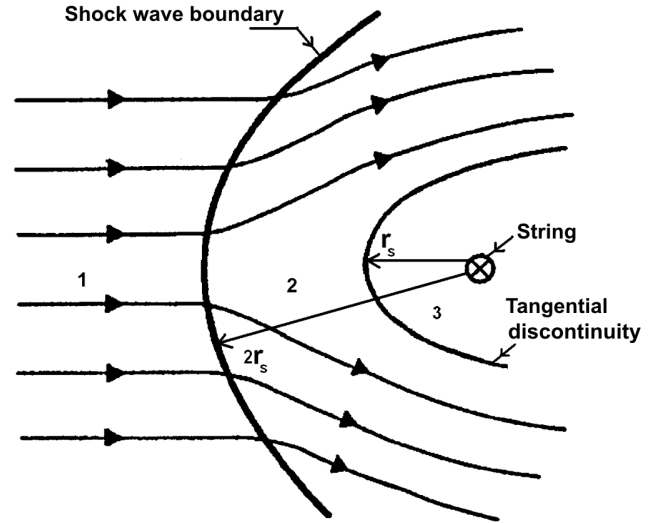


Fig. 1. Schematic diagram of a flow of the cosmic plasma near a superconducting string. The trajectories of particles of the plasma are marked by lines with arrows

the energy density e_2 behind the front of a shock wave are

$$n_2 \approx 4\gamma_2 n_1, \quad (7)$$

$$e_2 = e_{\text{tot}} \simeq e_p = \gamma_2 n_2 m_p c^2 \approx 4\gamma_2^2 n_1 m_p c^2. \quad (8)$$

The main contribution to the energy density behind the front of a relativistic shock wave is given by relativistic protons with $e_p \simeq e_2$. It is known from the analysis of data on ultrarelativistic waves in cosmological gamma-sparks [44] that the magneto-hydrodynamic (MHD) processes behind the front of a shock wave lead to the transfer of some part of the thermal energy of protons to electrons (so that $e_e = \epsilon_e e_2$) and to the generation of a turbulent magnetic field ($e_B = \epsilon_B e_2$), whose value

$$B_2 = 2\gamma_2 \sqrt{8\pi c^2 \epsilon_B m_p n_1} = 3.9 \times 10^{-5} \gamma_2 n_{-7}^{1/2} \epsilon_{B,-1}^{1/2} \text{ Gs} \quad (9)$$

exceeds significantly the value of the expected field in the case of its freezing. In this case, the energy densities of electrons and the magnetic field are essentially less than the energy density of protons ($\epsilon_B < 1$, $\epsilon_e < 1$).

Continuing the analogy with ultrarelativistic shock waves in gamma-ray bursts, we assume that the distribution of relativistic electrons in the after-shock region is a power one:

$$N(\gamma_e) = K' \gamma_e^{-p}, \quad (10)$$

($N(E_e) = KE_e^{-p}$). We set $p > 2$ ($p \approx 2.25$ for gamma-ray bursts).

The mean value of γ_e is

$$\langle \gamma_e \rangle = \frac{m_p}{m_e} \epsilon_e \gamma_2 \simeq \frac{m_p}{m_e} \epsilon_e \gamma_{\text{sh}}. \quad (11)$$

In this case, the concentration of electrons and the density of thermal energy of electrons are as follows:

$$n_{e,2} = \int_{E_{e,\min}}^{\infty} N(E_e) dE_e = \frac{K}{(p-1)E_{e,\min}^{(p-1)}}, \quad (12)$$

$$\begin{aligned} e_{e,2} &= \epsilon_e \gamma_2 n m_p c^2 = \int_{E_{e,\min}}^{\infty} N(E_e) E_e dE_e = \\ &= \frac{K}{(p-2)E_{e,\min}^{(p-2)}}. \end{aligned} \quad (13)$$

From the formulas for $e_{e,2}$ ($p \approx 2.2$, $\gamma_{\text{sh}} = 2$), we determined K :

$$\begin{aligned} K \frac{1 - (\frac{\gamma_{e,\min}}{\gamma_{e,\max}})^{p-2}}{(p-2)(\gamma_{e,\min} m_e c^2)^{p-2}} &= \epsilon_e \gamma_2 n_2 m_p c^2, \\ K &\simeq \epsilon_e 4 \gamma_2 (p-2) \gamma_2 n_1 m_p c^2 (m_e c^2 \gamma_{e,\min})^{p-2} = \\ &= 1.5 \times 10^{-12} \gamma_2^{2.2} n_{-7} \epsilon_{e,-1}^{1.2} \text{ erg}^{1.2} \text{ cm}^{-3}. \end{aligned} \quad (14)$$

$$K' = K / (m_e c^2)^{p-1} = 3 \times 10^{-5} \gamma_2^{2.2} n_{-7} \epsilon_{e,-1}^{1.2} \text{ cm}^{-3}. \quad (15)$$

The minimum Lorentz-factor of electrons

$$\gamma_{e,\min} = \frac{m_p}{m_e} \frac{p-2}{p-1} \gamma_2 \epsilon_e = 31 \gamma_2 \epsilon_{e,-1}. \quad (16)$$

The maximum Lorentz-factor can be estimated from the equality of the durations of the acceleration t_{acc} and the synchrotron cooling t_{syn} [46]:

$$t_{\text{acc}} = \frac{c R_L}{v_A^2}, \quad (17)$$

$$t_{\text{syn}} = \frac{\gamma_e m_e c^2}{P_{\text{syn}}}, \quad (18)$$

where $R_L = \gamma_e m_e c^2 / q_e B_2$ is the Larmor radius of an electron in the magnetic field B_2 , v_A is the Alfvén velocity, ($v_A^2 / c^2 \simeq 2 \epsilon_B$), $P_{\text{syn}} = \frac{4}{3} \sigma_T c \epsilon_B \gamma_e^2$ is the emission power of one electron in a local coordinate system

(the after-shock plasma), and σ_T is the Thompson cross-section. Finally, we get

$$\gamma_{e,\max} = \sqrt{\frac{12 \pi \epsilon_B q_e}{B_2 \sigma_T}} = 8.1 \times 10^9 \gamma_2^{-1/2} n_{-7}^{-1/4} \epsilon_{B,-1}^{1/4}. \quad (19)$$

Another limitation for $\gamma_{e,\max}$ accounts for the geometric boundedness of the acceleration region ($\sim r_s$): $E_{e,\max} = q_e r_s B_2$ or

$$\gamma_{e,\max} = q_e r_s B_2 / m_e c^2 \sim 7.1 \times 10^7 \gamma_2 \gamma_{\text{sh}}^{-1} k_i B_{-7} \alpha_{-8} \epsilon_{B,-1}^{1/2}. \quad (20)$$

Thus, due to the passage of a plasma across the front of a shock wave, we obtain the power spectrum of relativistic electrons with characteristics (10) and (15) and the maximum energy (19) or (20) behind the front. These electrons will manifest themselves due to the non-thermal emission from the after-shock region. Such an emission is one of the main manifestations of superconducting cosmic strings in the intergalactic plasma.

5. Synchrotron Emission of Electrons

The typical energy of synchrotron photons depends on the Lorentz-factor γ_e of relativistic electrons and on a magnetic field strength and is equal to (in a local coordinate system)

$$\hbar \omega_{\text{syn}} = \frac{\hbar q_e B_2}{m_e c} \gamma_e^2, \quad (21)$$

whereas the observed duration of the cooling is given by formula (18). Therefore, the duration of the cooling as a function of the energy of photons can be written as

$$t_{\text{syn}}(\nu_{\text{syn}}) = \frac{3}{\sigma_T} \sqrt{\frac{2 \pi c m_e q_e}{B_2^3 \nu_{\text{syn}}}}. \quad (22)$$

The critical parameter determining the mode of cooling (fast or slow) is the Lorentz-factor $\gamma_{e,c}$ of electrons which are cooled for the hydrodynamic time. We will find it from the comparison of the hydrodynamic time of the system $t_{\text{hyd}} \sim r_{\text{sh}} / c$ and the time of the synchrotron cooling t_{syn} :

$$\begin{aligned} \gamma_{e,c} &= \frac{3 m_e c}{4 \sigma_T \epsilon_B t_{\text{hyd}}} \approx \\ &\approx 7 \times 10^{12} \gamma_2^{-1} k_i^{-1} \alpha_{-8}^{-1} B_{-7}^{-1} n_{-7}^{-1/2} \epsilon_{B,-1}^{-1}. \end{aligned} \quad (23)$$

The fast cooling is realized if $\gamma_{e,c} < \gamma_{e,\min}$, i.e. all electrons rapidly loss their energy for the emission. But if $\gamma_{e,c} > \gamma_{e,\min}$, then only a part of electrons above $\gamma_{e,c}$ is efficiently cooled, and the main amount of electrons is in the mode of slow cooling.

As was shown in [46], the synchrotron emission from the power distribution can be approximated by the broken energy spectrum with three characteristic frequencies of breaks. The first is the self-absorption frequency ν_a , below which the system becomes optically thick. At the frequencies $\nu_a \geq \nu$, the self-absorption is important, and the emission flow is proportional to ν^2 . Two other characteristic frequencies ν_m and ν_c correspond to the emission of electrons with the Lorentz-factor $\gamma_{e,\min}$ and γ_c , respectively. In our case, $\nu_a < \nu_m < \nu_c$.

For the energy spectrum of electrons (11), the energy of the synchrotron emission from unit volume per unit frequency interval (spectral emissive ability) for slow cooling can be written as

$$j_\nu \sim \begin{cases} (\nu/\nu_m)^2 j_{\nu,\max}, & \text{if } \nu_a \geq \nu; \\ (\nu/\nu_m)^{1/3} j_{\nu,\max}, & \text{if } \nu_m \geq \nu > \nu_a; \\ (\nu/\nu_m)^{-(p-1)/2} j_{\nu,\max}, & \text{if } \nu_c \geq \nu > \nu_m; \\ (\nu_c/\nu_m)^{-(p-1)/2} (\frac{\nu}{\nu_c})^{-p/2} j_{\nu,\max}, & \text{if } \nu > \nu_c. \end{cases} \quad (24)$$

In a local reference system, the characteristic frequency of the synchrotron emission of an electron which moves with γ_e

$$\nu_{\text{syn}} = \frac{q_e B_2}{2\pi m_e c} \gamma_e^2. \quad (25)$$

The emission power maximum is observed at the frequency (for an electron with $\gamma_{e,\min}$)

$$\nu_m \approx \frac{q_e B_2}{4\pi m_e c} \gamma_{e,\min}^2 = 5.3 \times 10^4 \gamma_2^3 n_{-7}^{1/2} \epsilon_{e,-1}^{1/2} \epsilon_{B,-1} \text{ Hz}. \quad (26)$$

For the mode of slow cooling (here and below, we take

Table 2. Maxima of the flows of the synchrotron, synchrotron self-Compton, and inverse Compton emissions from loops at the mean distance from the observer (for $n_1 = 10^{-7} \text{ cm}^{-3}$, $B_1 = 10^{-7} \text{ Gs}$, $\epsilon_e = 0.1$, $\epsilon_B = 0.1$, $\gamma_{\text{sh}} = 2$)

| α | Flows, (erg/cm ² · Hz · s) | | |
|-------------------|---------------------------------------|-----------------------------|----------------------------|
| | $F_{\nu,\max}$ | $F_{\nu,\max}^{\text{SSC}}$ | $F_{\nu,\max}^{\text{IC}}$ |
| 10 ⁻⁶ | 1.1 × 10 ⁻²⁶ | 1.5 × 10 ⁻⁴⁰ | 2.1 × 10 ⁻⁴⁰ |
| 10 ⁻⁸ | 2.4 × 10 ⁻³¹ | 3.3 × 10 ⁻⁴⁷ | 4.5 × 10 ⁻⁴⁵ |
| 10 ⁻¹¹ | 2.4 × 10 ⁻³⁸ | 3.3 × 10 ⁻⁵⁷ | 4.5 × 10 ⁻⁵² |

$p = 2.2$),

$$j_{\nu,\max} = AK' \nu_m^{\frac{-(p-1)}{2}} = 3.6 \times 10^{-31} \gamma_2^{3.2} n_{-7}^{3/2} \epsilon_{B,-1}^{1/2} \epsilon_{e,-1}^{1.2} \text{ erg/cm}^3 \cdot \text{Hz} \cdot \text{c}, \quad (27)$$

where we used the formula [47]

$$A = \Gamma \left(\frac{p}{4} + \frac{19}{12} \right) \Gamma \left(\frac{p}{4} - \frac{1}{12} \right) \frac{\sqrt{3\pi} \Gamma(\frac{p+5}{4}) q_e^3 B_2}{\Gamma(\frac{p+7}{4}) (p-1) m_e c^2} \times \left(\frac{2\pi m_e c}{3q_e B_2} \right)^{\frac{-(p-1)}{2}}. \quad (28)$$

The spectral flow of the synchrotron emission

$$F_\nu = \frac{V_{\text{em}} j_\nu}{4\pi d_s^2}, \quad (29)$$

where V_{em} is the volume of the radiating region, and d_s is the mean distance from the Earth's observer to the string. Let the cross-section and the length of the radiating region be r_s and l , respectively. Then $V_{\text{em}} = \frac{3}{2} \pi r_s^2 l \approx 2 \times 10^{-4} \gamma_{\text{sh}}^{-2} k_i^2 B_{-7}^2 \alpha_{-8}^3 n_{-7}^{-1} \text{ pc}^3$.

The maximum of a synchrotron emission flow (erg/cm² · Hz · s) (see Tables 2, 3 and Fig. 2):

$$F_{\nu,\max} = 2.1 \times 10^{-31} \gamma_2^{3.2} \gamma_{\text{sh}}^{-2} k_i^2 B_{-7}^2 \alpha_{-8}^{7/3} n_{-7}^{1/2} \epsilon_{B,-1}^{1/2} \epsilon_{e,-1}^{1.2}. \quad (30)$$

6. Synchrotron Self-Compton Emission

New-born synchrotron photons can scattered by relativistic electrons behind the front of a shock wave. With regard for the fact that the electrons are ultrarelativistic (their energy \gg the energy of photons), the inverse Compton effect will be observed under the scattering: the electrons will transfer the energy to photons. The inverse Compton scattering by "own" synchrotron

Table 3. Estimation of the flow in unit logarithmic frequency interval $\nu_m F_{\nu,\max}$, $\nu_m^{\text{SSC}} F_{\nu,\max}^{\text{SSC}}$, $\nu_m^{\text{IC}} F_{\nu,\max}^{\text{IC}}$ from strings at the mean distance from the observer (for $n_1 = 10^{-7} \text{ cm}^{-3}$, $B_1 = 10^{-7} \text{ Gs}$, $\epsilon_e = 0.1$, $\epsilon_B = 0.1$, $\gamma_{\text{sh}} = 2$)

| α | Flows, (erg/cm ² · s) | | |
|-------------------|----------------------------------|--|--|
| | $\nu_m F_{\nu,\max}$ | $\nu_m^{\text{SSC}} F_{\nu,\max}^{\text{SSC}}$ | $\nu_m^{\text{IC}} F_{\nu,\max}^{\text{IC}}$ |
| 10 ⁻⁶ | 2.4 × 10 ⁻²¹ | 3.4 × 10 ⁻³¹ | 4.4 × 10 ⁻²⁶ |
| 10 ⁻⁸ | 5.1 × 10 ⁻²⁶ | 7.4 × 10 ⁻³⁸ | 9.4 × 10 ⁻³¹ |
| 10 ⁻¹¹ | 5.1 × 10 ⁻³³ | 7.4 × 10 ⁻⁴⁸ | 9.4 × 10 ⁻³⁸ |

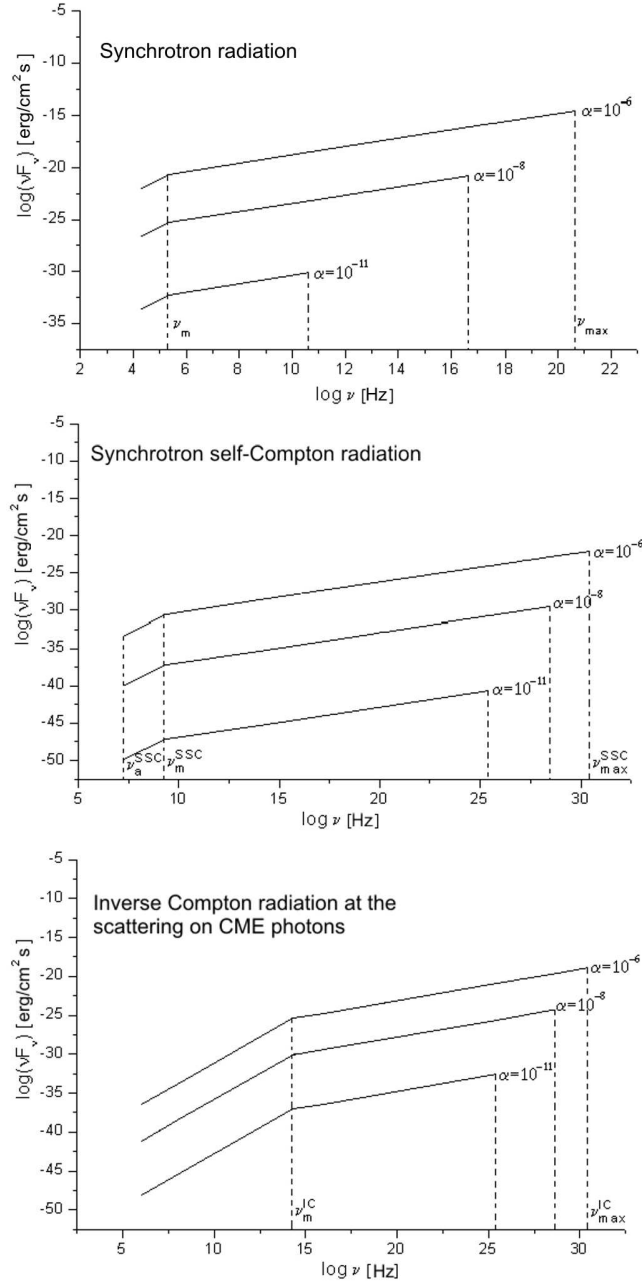


Fig. 2. Expected flows of the synchrotron, synchrotron self-Compton, and inverse Compton emissions of relativistic electrons behind the front of a shock wave for loops with various tensions (linear density) at the mean distance from the Earth's observer (for $n_1 = 10^{-7} \text{ cm}^{-3}$, $B_1 = 10^{-7} \text{ Gs}$, $\epsilon_e = 0.1$, $\epsilon_B = 0.1$, $\gamma_{sh} = 2$)

photons is called the synchrotron self-Compton emission (as distinct, e.g., from “ordinary” inverse Compton scattering by relic photons). There are known the different modes of the inverse Compton effect [46]:

1) $E_{\text{syn}}\gamma_{e,\text{min}} \leq m_e c^2$ – Thompson limit, for which $E_{\text{IC}} = E_{\text{syn}}\gamma_e^2$; 2) $E_{\text{syn}}\gamma_{e,\text{min}} \gg m_e c^2$ – Klein–Nishina limit, for which $E_{\text{IC}} = \frac{4}{3}E_{\text{syn}}\gamma_e$.

By using the synchrotron spectrum, we can calculate the spectrum of the self-Compton emission, by integrating the former over the distribution of electrons [46]:

$$F_\nu^{\text{SSC}} = r_s \sigma_T \int_{\gamma_{e,\text{min}}}^{\infty} d\gamma_e N(\gamma_e) \int_0^{x_0} dx F_\nu(x), \quad (31)$$

where $x = \nu/4\gamma_e^2\nu_{\text{syn}}$ ($x_0 = 0.5$). Analogously to the spectrum of the synchrotron emission, the spectrum of the self-Compton emission with characteristic values $\nu^{\text{SSC}} = 4\gamma_e^2\nu_{\text{syn}}x_0$ is composed of several segments with breaks.

For the mode of slow cooling, we have

$$F_\nu^{\text{SSC}} = x_0 r_s \sigma_T n_2 F_\nu(\nu_{\text{syn}}(\gamma_{e,\text{min}})) \times \quad (32)$$

$$\times \begin{cases} \frac{5}{2} \frac{(p-1)}{(p+1)} \left(\frac{\nu_a}{\nu_m}\right)^{1/3} \left(\frac{\nu}{\nu_a^{\text{SSC}}}\right), & \text{if } \nu \leq \nu_a^{\text{SSC}}; \\ \frac{3}{2} \frac{(p-1)}{(p-1/3)} \left(\frac{\nu}{\nu_m^{\text{SSC}}}\right)^{1/3}, & \text{if } \nu_a^{\text{SSC}} < \nu \leq \nu_m^{\text{SSC}}; \\ \frac{(p-1)}{(p+1)} \left(\frac{\nu}{\nu_m^{\text{SSC}}}\right)^{\frac{1-p}{2}} \left[\frac{4(p+1/3)}{(p+1)(p-1/3)} + \ln\left(\frac{\nu}{\nu_m^{\text{SSC}}}\right) \right], & \text{if } \nu_m^{\text{SSC}} < \nu \leq \sqrt{\nu_m^{\text{SSC}}\nu_c^{\text{SSC}}}; \\ \frac{(p-1)}{(p+1)} \left(\frac{\nu}{\nu_m^{\text{SSC}}}\right)^{\frac{1-p}{2}} \left[2\frac{(2p+3)}{(p+2)} - \frac{2}{(p+1)(p+2)} + \ln\left(\frac{\nu_c^{\text{SSC}}}{\nu}\right) \right], & \text{if } \sqrt{\nu_m^{\text{SSC}}\nu_c^{\text{SSC}}} < \nu \leq \nu_c^{\text{SSC}}; \\ \frac{(p-1)}{(p+1)} \left(\frac{\nu}{\nu_m^{\text{SSC}}}\right)^{\frac{-p}{2}} \left(\frac{\nu_c}{\nu_m}\right) \left[2\frac{(2p+3)}{(p+2)} + \frac{2}{(p+2)^2} + \frac{(p+1)}{(p+2)} \ln\left(\frac{\nu}{\nu_c^{\text{SSC}}}\right) \right], & \text{if } \nu > \nu_c^{\text{SSC}}. \end{cases}$$

The maximum of the emission flow ($\text{erg/cm}^2 \cdot \text{Hz} \cdot \text{s}$) (see Tables 2, 3 and Fig. 2):

$$F_{\nu,\text{max}}^{\text{SSC}}(\nu_m^{\text{SSC}}) \simeq 4\sigma_T r_s n_2 x_0 \frac{(p-1)(p+1/3)}{(p-1/3)(p+1)^2} F_{\nu,\text{syn}}(\nu_B) = 3.7 \times 10^{-47} \gamma_2^{4.2} \gamma_{sh}^{-3} k_i^3 B_{-7}^3 \alpha_{-8}^{10/3} n_{-7} \epsilon_{B,-1}^{1/2} \epsilon_{e,-1}^{1.2} \quad (33)$$

in the case where $\nu_a^{\text{SSC}} \ll \nu_m^{\text{SSC}} \ll \nu_c^{\text{SSC}}$.

The emission frequency:

$$\nu_m^{\text{SSC}} = 4\gamma_{e,\text{min}}^2 \nu_m = 2.1 \times 10^8 \gamma_2^5 n_{-7}^{1/2} \epsilon_{e,-1}^4 \epsilon_{B,-1}^{1/2} \text{ Hz.} \quad (34)$$

7. Inverse Compton Effect on CMB photons

High-energy electrons of the cosmic plasma can be also scattered on CMB photons, by transferring them a part of their energy. We now calculate the spectrum of Compton photons under the scattering of relativistic electrons on the black-body emission with the temperature $T = 2.7$ K (on photons of the cosmic microwave emission).

Under the inverse Compton emission in the Thompson mode, the spectral emissive ability can be written as [48]

$$j_{\nu}^{\text{IC}} = K' \frac{8\pi^2 r_e^2}{h^2 c^2} (kT)^{(p+5)/2} F(p) (h\nu)^{-(p-1)/2}. \quad (35)$$

Here, $h = 2\pi\hbar$, k – Boltzmann's constant, r_e – electron radius ($r_e = q_e^2/m_e c^2$), and the function

$$F(p) = 2^{p+3} \frac{p^2 + 4p + 11}{(p+3)^2(p+5)(p+1)} \Gamma\left(\frac{p+5}{2}\right) \zeta\left(\frac{p+5}{2}\right). \quad (36)$$

The frequency corresponding to the emissive ability maximum:

$$\nu_m^{\text{IC}} = \gamma_{e,\min}^2 \frac{3kT}{2h} = 8.1 \times 10^{13} \gamma_2^2 \epsilon_{e,-1}^2 \text{ Hz}. \quad (37)$$

The emissive ability maximum for the inverse Compton emission:

$$j_{\nu,\max}^{\text{IC}}(\nu_m^{\text{IC}}) = 1.9 \times 10^{-44} \gamma_2 n_{-7} \text{ erg/cm}^3 \cdot \text{Hz} \cdot \text{s}. \quad (38)$$

The maximum of the emission flow from the string at the mean distance from the Earth's observer ($\text{erg/cm}^2 \cdot \text{Hz} \cdot \text{s}$) (see Tables 1, 2 and Fig. 2):

$$F_{\nu,\max}^{\text{IC}}(\nu_m^{\text{IC}}) = 1.1 \times 10^{-44} \gamma_2 \gamma_{\text{sh}}^{-2} k_i^2 B_{-7}^2 \alpha_{-8}^{7/3}. \quad (39)$$

Since the maximum energy of accelerated electrons of the order of 10^{15} eV, the maximum energy of synchrotron emission is of the order of 10^6 eV. That is, the synchrotron spectrum extends to the hard X-ray- and gamma-ranges with the maximum flow $\nu_{\max} F_{\nu}(\nu_{\max}) \sim 10^{-15}$ ($\text{erg/cm}^2 \cdot \text{s}$). At the same time, the sensitivity of modern X-ray telescopes in this range is also of the order $\nu F_{\nu} \sim 10^{-15}$ ($\text{erg/cm}^2 \cdot \text{s}$) (for comparison, ACIS on Chandra can registered flows less than 4×10^{-15} ($\text{erg/cm}^2 \cdot \text{s}$) for the energies of 0.4–6 keV). The result allows one to see a cosmic loop with $\alpha = 10^{-6}$ in the X-ray-range even at the mean distance from the observer.

In our model, the maximum energy of inverse Compton emission is of the order of 10^{13} eV. That is, the

spectrum extends to the TeV-range with the maximum flow $\nu_{\max}^{\text{IC}} F_{\nu}^{\text{IC}}(\nu_{\max}^{\text{IC}}) \sim 10^{-20}$ ($\text{erg/cm}^2 \cdot \text{s}$). At the same time, the sensitivity of modern Cherenkov telescopes in this range is of the order $\nu F_{\nu} \sim 10^{-13}$ ($\text{erg/cm}^2 \cdot \text{s}$). Therefore, a cosmic loop can be seen in the TeV-range only from a distance less than 100 kpc.

Generally, the flows of the synchrotron and inverse Compton emissions from a cosmic loop at the typical distance from the Earth which are calculated in the present work are lower the sensitivity of available facilities. Therefore, we may hope for the observation of a loop only if it is sufficiently close to the Earth. At the same time, we do not consider the possible collimation and increase of the flow from sections of loops which move with a high Lorentz-factor. In particular, the near-cusp regions will emit significantly more powerful flows.

8. Conclusions

In the present work, we have considered the astrophysical manifestations of superconducting cosmic strings due to the nonthermal emission of electrons of the cosmic plasma accelerated on the front of a shock wave near the magnetosphere of a string. It is shown that the superconducting strings in the magnetized intergalactic medium can be powerful sources of the nonthermal emission. We have calculated the flows and spectra of the synchrotron, synchrotron self-Compton, and inverse Compton emissions of relativistic electrons under their scattering on relict photons. Modern X-ray- and gamma-telescopes can register such loops at a relatively small distance from the Earth, about 0.1 Mpc. However, the near-cusp regions can generate significantly more powerful, though, respectively, essentially collimated and therefore less frequent impulses, whose study will be performed elsewhere.

This work was partially supported by the Swiss National Science Foundation and the Swiss Agency for Development and Cooperation in the framework of the program SCOPEs. The work of B. Hnatyk was supported by program “Kosmomikrofizyka” of the NASU.

1. T.W.B. Kibble, *J. Phys. A* **9**, 1387 (1976).
2. Ya.B. Zeldovich, *Mon. Not. Roy. Astron. Soc.* **192**, 663 (1980).
3. A. Vilenkin, *Phys. Rev. Lett.* **46**, 1169 (1981) [Erratum: *Ibid.* **46**, 1496 (1981)]
4. E. Witten, *Phys. Lett. B* **153**, 243 (1985).

5. E.J. Copeland, R.C. Myers, and J. Polchinski, *JHEP* **0406**, 013 (2004) [arXiv:hep-th/0312067].
6. S. Sarangi and S.H.H. Tye, *Phys. Lett. B* **536**, 185 (2002) [arXiv:hep-th/0204074].
7. R. Jeannerot, *Phys. Rev. D* **53**, 5426 (1996) [arXiv:hep-ph/9509365].
8. R. Jeannerot, J. Rocher, and M. Sakellariadou, *Phys. Rev. D* **68**, 103514 (2003) [arXiv:hep-ph/0308134].
9. N. Turok and R.H. Brandenberger, *Phys. Rev. D* **33**, 2175 (1986).
10. H. Sato, *Prog. Theor. Phys.* **75**, 1342 (1986).
11. A. Stebbins, *Ap. J. (Lett.)* **303**, L21 (1986).
12. R.H. Brandenberger, *Int. J. Mod. Phys. A* **9**, 2117 (1994) [arXiv:astro-ph/9310041].
13. M. Wyman, L. Pogosian, and I. Wasserman, *Phys. Rev. D* **72**, 023513 (2005) [Erratum: *Ibid. D* **73**, 089905 (2006)] [arXiv:astro-ph/0503364].
14. A.A. Fraisse, [arXiv:astro-ph/0503402].
15. S. Amsel, J. Berger, and R.H. Brandenberger, [arXiv:astro-ph/0709.0982].
16. A.A. Fraisse, C. Ringeval, D.N. Spergel, and F.R. Bouchet, [arXiv:astro-ph/0708.1162].
17. L. Pogosian, S.-H.H. Tye, I. Wasserman, and M. Wyman, [arXiv:astro-ph/0804.0810v1].
18. A.A. Fraisse, C. Ringeval, D.N. Spergel, and F.R. Bouchet, [arXiv:astro-ph/0708.1162v1].
19. A.A. Fraisse, *JCAP* **0703**, 008, (2007), [arXiv:astro-ph/0603589v2].
20. F. Dubath, J. Polchinski, and J.V. Rocha, [arXiv:astro-ph/0711.0994v2].
21. V. Vanchurin, [arXiv:gr-qc/0712.2236v2].
22. A. Vilenkin and E.P.S. Shellard; *Cosmic Strings and Other Topological Defects*, (Cambridge Univ. Press, Cambridge, 1994).
23. T. Damour and A. Vilenkin, *Phys. Rev. D* **71**, N063510 (2005).
24. A. Vilenkin, *Astrophys. J.* **282**, L51 (1984).
25. C. Hogan and R. Narayan, *MNRAS* **211**, 575 (1984).
26. L. Cowie and E. Hu, *Astrophys. J. (Lett.)* **318**, L33 (1987).
27. A. A. de Laix, [arXiv:astro-ph/9705223v1].
28. F. Bernardeau and J. Uzan, [arXiv:astro-ph/0004102].
29. M. Sazhin *et al.*, *Mon. Not. Roy. Astron. Soc.* **343**, 353 (2003), [arXiv:astro-ph/0302547].
30. M.V. Sazhin, M. Capaccioli, G. Longo, M. Paolillo, and O. S. Khovanskaya, [arXiv:astro-ph/0601494].
31. R. Schild, I.S. Masnyak, and B.I. Hnatyk, [arXiv:astro-ph/0406434].
32. C. Ringeval, [arXiv:hep-ph/0106179].
33. F. Ferrer, H. Mathur, T. Vachaspati, and G. Starkman, [arXiv:hep-th/0602132 v1].
34. P. Peter, (DAMTP-93/34) [arXiv:hep-th/9312280].
35. A. Vilenkin and T. Vachaspati, *Phys. Rev. Lett.* **58**, 1041 (1987).
36. V. Berezhinsky, B. Hnatyk, and A. Vilenkin, *Phys. Rev. D* **64**, 3004 (2001).
37. D.R. Lorimer, M. Bailes, M.A. McLaughlin, D.J. Narkevic, and F. Crawford, [arXiv:astro-ph/0709.4301].
38. T. Vachaspati, [arXiv:astro-ph/0802.0711v3].
39. E.M. Chudnovsky, G.B. Field, D.N. Spergel, and A. Vilenkin, *Phys. Rev. D* **34**, 4 (1986).
40. M. Sakellariadou, [arXiv:hep-th/0802.3379v1].
41. C. Ringeval, M. Sakellariadou, and F. Bouchet, *JCAP* **0702**, 023 (2007) [arXiv:astro-ph/0511646].
42. X. Siemens, J. Creighton, Ir. Maor, S.R. Majumder, K. Cannon, and J. Read, *Phys. Rev. D* **73**, 10, 105001, (2006), [arXiv:gr-qc/0603115v1].
43. E. Witten, *Nuclear Physics B* **249**, 557 (1985).
44. G.V. Bicknell, S.J. Wagner, and B.A. Groves, [arXiv:astro-ph/0103200].
45. T. Piran, *Phys. Rep.* **314**, 575 (1999); [arXiv:astro-ph/9810256].
46. R. Sari and A.A. Esin, *ApJ* **548**, 787 (2001); [arXiv:astro-ph/0005253].
47. G. B. Rybicki and A. P. Lightman, *it Radiative Processes in Astrophysics* (Wiley, New York, 1979).
48. B. Katz and E. Waxman, *JCAP* **0801**, 018 (2008), [arXiv:astro-ph/0706.3485v3].

Одержано 16.08.08.

Translated from Ukrainian by V.V. Kukhtin

ЕЛЕКТРОМАГНІТНЕ ВИПРОМІНЮВАННЯ
КОСМІЧНИХ СТРУН

Л.В. Задорожна, Б.І. Гнатик

Резюме

Космічні струни – один з видів топологічних дефектів, що утворюються під час фазових переходів полів зі спонтанним порушенням симетрії у ранньому Всесвіті. Особливий інтерес

представляють надпровідні космічні струни, всередині котрих без опору рухаються безмасові носії заряду. В роботі показано, що надпровідні космічні струни у міжгалактичному магнітному полі можуть бути джерелами потужного нетеплового випромінювання. Розраховано спектри синхротронного, синхротронного само-комптонівського та оберненого комптонівського

випромінювання релятивістських електронів, прискорених на фронті ударної хвилі навколо струни. Сучасними рентгеновськими та гама-телескопами можливо виявити петлі на досить невеликій відстані – до 0,1 Мпк. Тим не менше, від прикаспових областей можуть очікуватися набагато потужніші, проте суттєво колімовані імпульси.